ISSN 1949-8470 (online)

World Journal of *Radiology*

World J Radiol 2017 August 28; 9(8): 321-338

Published by Baishideng Publishing Group Inc

World Journal of Radiology

Contents

Monthly Volume 9 Number 8 August 28, 2017

World Journal of Radiology
Volume 9 Number 8 August 28, 2017

Contents

NAME OF JOURNAL
World Journal of Radiology

ISSN
ISSN 1949-8470 (online)

LAUNCH DATE
January 31, 2009

FREQUENCY
Monthly

EDITORIAL OFFICE
Xiu-Xia Song, Director
World Journal of Radiology
Baishideng Publishing Group Inc
7901 Stoneridge Drive, Suite 501, Pleasanton, CA 94588, USA
Telephone: +1-925-2238242
Fax: +1-925-2238243
E-mail: editorialoffice@wjgnet.com
Help Desk: http://www.f6publishing.com/helpdesk
http://www.wjgnet.com

PUBLISHER
Baishideng Publishing Group Inc
7901 Stoneridge Drive, Suite 501,
Pleasanton, CA 94588, USA
Telephone: +1-925-2238242
Fax: +1-925-2238243
E-mail: bpgoffice@wjgnet.com
Help Desk: http://www.f6publishing.com/helpdesk
http://www.wjgnet.com

PUBLICATION DATE
August 28, 2017

World Journal of Radiology

Submit a Manuscript: http://www.f6publishing.com

World J Radiol 2017 August 28; 9(8): 330-338

DOI: 10.4329/wjr.v9.i8.330

ISSN 1949-8470 (online)

ORIGINAL ARTICLE

Observational Study

Clinical-radiological-pathological correlation of cavernous sinus hemangioma: Incremental value of diffusion-weighted imaging

Abhishek Mahajan, Vedula Rajni Kanth Rao, Gudipati Anantaram, Ashwin M Polnaya, Sandeep Desai, Paresh Desai, Rammohan Vadapalli, Manas Panigrahi

Abhishek Mahajan, Ashwin M Polnaya, Department of Radio-diagnosis, Tata Memorial Centre, Mumbai 400012, India

Vedula Rajni Kanth Rao, Gudipati Anantaram, Department of Radiology, Krishna Institute of Medical Sciences, Secunderabad 500003, India

Sandeep Desai, Department of Radiodiagnosis Clumax Imaging, Bangalore 560011, India

Paresh Desai, Department of Radiology, Apollo Victor Hospital, Goa 403601, India

Rammohan Vadapalli, Department of Radiology, Vijaya Diagnostics, Hyderabad, Secunderabad 500003, India

Manas Panigrahi, Department of Neurosurgery, Krishna Institute of Medical Sciences, Secunderabad 500003, India

Author contributions: Guarantors of integrity of entire study by all authors; study concepts/study design or data acquisition or data analysis/interpretation by all authors; manuscript drafting or manuscript revision for important intellectual content by all authors; manuscript final version approval by all authors; literature research by all authors; manuscript editing by all authors; all authors take responsibility for the integrity of the data and the accuracy of the data analysis.

Institutional review board statement: The study was reviewed and approved by the Institutional review board.

Informed consent statement: Participants gave informed consent for data sharing.

Conflict-of-interest statement: I confirm that this manuscript is not published anywhere else and on behalf of all authors, I state that there is no conflict of interests (including none for related to commercial, personal, political, intellectual, or religious interests).

Data sharing statement: All the cases presented in this article belong to the authors and have not been copied or borrowed from any published material. Technical appendix, statistics, and dataset available from the corresponding author Dr V R K Rao (vedula@gmail.com). The authors whose names are listed above certify that they have no affiliations with or involvement in any organization or entity with any financial interest or non-financial interest in the subject matter or materials discussed in this manuscript. The authors certify that a manuscript on the same or similar material has not already been published or has not been or will not be submitted to another journal or by colleagues at their institution before their work appears in your journal.

Manuscript source: Invited manuscript

Correspondence to: Vedula Rajni Kanth Rao, MD, DMRD, Department of Radiology, Krishna Institute of Medical Sciences, Minister Road, Secunderabad 500003, India. drvedula@kimshospitals.co.in
Telephone: +91-99-89773473
Fax: +91-40-27840980

Received: February 21, 2017
Peer-review started: February 26, 2017
First decision: March 27, 2017
Revised: May 8, 2017
Accepted: May 22, 2017
Article in press: May 24, 2017
Published online: August 28, 2017

Abstract

AIM

To elucidate the clinical, magnetic resonance imaging (MRI), pathological features of these lesions and asses the incremental value of diffusion-weighted imaging (DWI) in diagnosing them.

METHODS

Fifteen consecutive patients (11 females and 4 males; mean age 40.93 years; age range 13-63 years) with cavernous sinus hemangiomas (CSH) who underwent examination between November 2008 and May 2016 were included for the analysis. MRI, clinical and surgical findings of each patient was retrospectively reviewed. DWI were also analysed and mean-apparent diffusion coefficient (ADC) value was calculated. Eleven patients underwent surgical removal of the lesion and 2 patients had biopsy only. Diagnosis of CSH was confirmed histologically in 13 patients.

RESULTS

Eleven patients (73%) presented with headaches and 10 (66%) had cranial nerve involvement. Extra cavernous sinus extension was noted in 14 (94%). Surgery was performed in 13 (87%) and post-operative radiation was given to 4 (28%) patients. Thirteen patients remained asymptomatic on follow up. Three conspicuous imaging features were highly suggestive of the diagnosis: Lack of diffusion restriction (100%), homogeneous hyperintensity on T2 weighted image sequences (93.3%) and intense post-contrast enhancement (100%). The mean ADC was $1.82 \times 10^{-3} \pm 0.2186$ cm^2/s.

CONCLUSION

T1-weighted hypointensity with homogeneous hyperintensity on T2-weighted sequences, intense enhancement and absence of hemosiderin within the lesion on GRE sequence favour the diagnosis. Facilitated diffusion on DWI differentiates CSH from other solid cavernous sinus lesions and significantly improves the diagnostic accuracy, a critical factor for planning surgery.

Key words: Cavernous sinus hemangioma; Cavernous sinus; Magnetic resonance imaging; Diffusion weighted imaging

Core tip: Cavernous hemangioma in the cavernous sinus are rare lesions with significant female preponderance. This article highlights the diagnostic magnetic resonance imaging features of cavernous sinus hemangiomas (CSH). T1-weighted hypointensity with homogeneous hyperintensity on T2-weighted sequence, absence of hemosiderin within the lesion on GRE sequence and intense post contrast enhancement favour the diagnosis. On diffusion-weighted imaging CSH shows facilitated diffusion and is nearly 100% specific for CSH. Markedly hypointense hemangioma on T1 weighted images suggests schirrous nature of the lesion and is amenable to complete surgical excision.

Mahajan A, Rao VRK, Anantaram G, Polnaya AM, Desai S, Desai P, Vadapalli R, Panigrahi M. Clinical-radiological-pathological correlation of cavernous sinus hemangioma: Incremental value of diffusion-weighted imaging. *World J Radiol* 2017; 9(8): 330-338 Available from: URL: http://www.wjgnet.com/1949-8470/full/v9/i8/330.htm DOI: http://dx.doi.org/10.4329/wjr.v9.i8.330

INTRODUCTION

Cavernous hemangioma in the cavernous sinus has an estimated prevalence of 1% incidence with significant female preponderance, considered to be due to hormonal influence[1,2]. The lesion is rare in occurrence closely mimicking commonly encountered cavernous sinus lesions such as schwannoma, meningioma, chordoma, granuloma, carotid aneurysm and lymphoproliferative conditions[3,4]. Microscopically cavernous sinus hemangioma (CSH) consists of multiple vascular channels lined by a single layer of endothelium without muscular layer and any intervening neural tissue[2]. Magnetic resonance imaging (MRI) is the imaging modality of choice for evaluating cavernous sinus lesions. On MR imaging, CSH shows hypointense signal on T1 weighted images (T1-W) and hyperintense signal on T2 weighted images (T2-W) that is indistinguishable from the other lesions which have high cellular matrix and/or necrotic components[3,4]. T2 prolongation resulting in extremely high signal intensity has been considered a definite sign of a cavernous hemangioma[4,5]. Hence, even at MRI, the diagnosis of a cavernous hemangioma can still be in doubt, with the main differential diagnosis being a schwannoma of the V nerve or meningioma[3,6]. The study aimed to elucidate the clinical, MRI, pathological features of these lesions and asses the incremental value of diffusion-weighted imaging (DWI) in diagnosing them.

MATERIALS AND METHODS

This retrospective interpretation of data was approved by the hospital internal review board and informed consent was waived. A total of 15 consecutive patients with CSH who underwent MRI examination between December 2008 and May 2016 were included for the analysis. MRI, clinical, and surgical findings of each patient were retrospectively reviewed. Imaging was performed on both 1.5-T and 3-T systems (HDxt GE, Siemens Medical, Philips Ingenia) using 8 channel high resolution dedicated brain coil. The imaging protocol included spin-echo T1-W, fast spin-echo T2-W, fluid-attenuated inversion recovery imaging (FLAIR) and contrast-enhanced spin-echo T1-W was performed following gadolinium injection. Fast Imaging Employing

Table 1 Signal intensities and other features on conventional and special magnetic resonance imaging sequences

Case No.	T1W	T2W	T2 FLAIR	Post-contrast	Flow voids	Extension beyond cavernous sinus	Vessel encasement	DWI	Blooming on GRE
1	Hypo	Hyper	Hyper	Intense enhancement	Yes	Moderate	Yes	Hypointense	No
2	Hypo	Hyper	Hyper	Intense enhancement	No	Moderate	Yes	Hypointense	No
3	Hypo	Hyper	Hyper	Intense enhancement	No	Moderate	Yes	Hypointense	No
4	Hypo	Hyper	Hyper	Intense enhancement	No	Extensive	Yes	Not done	No
5	Hypo	Hyper	Hyper	Intense enhancement	No	Extensive	Displaced only	Hypointense	Not done
6	Hypo	Hyper	Hyper	Intense enhancement	No	Nil	Displaced only	Not done	Not done
7	Hypo	Hyper	Hyper	Intense enhancement	Yes	Mild	Yes	Hypointense	No
8	Hypo	Hyper	Hyper	Intense enhancement	Centripetal filling	Moderate	Yes	Hypointense	-
9	Iso intense	Mildly hyper	Not done	Intense enhancement	No	Moderate	Yes	Hypointense	Not done
10	Hypo	Hyper	Not done	Intense enhancement	No	Mild	Yes	Not done	Not done
11	Hypo	Hyper	Hyper	Not available	No	Moderate	No	Not done	Not done
12	Hypo	Hyper	Hyper	Intense enhancement	Vascular supply from left ICA	Extensive	Yes	Hypointense	No
13	Hypo	Hyper	Hyper	Intense enhancement	No	Mild	Yes	Hypointense	No
14	Hypo	Hyper	Hyper	Intense enhancement	No	Extensive	Yes	Hypointense	Not done
15	Hypo	Hyper	Hyper	Intense enhancement	Yes	Extensive	Yes	Not done	Not done

T1-W: T1 weighted image; T2-W: T2 weighted image; FLAIR: Fluid attenuated inversion recovery; DWI: Diffusion-weighted imaging; GRE: Gradient recalled echo.

Steady-state Acquisition (FIESTA) and susceptibility weighted imaging (SWI) were added to the routine sequences in two patients. Diffusion weighted imaging was performed in ten patients and GRE imaging in seven. MR angiography and digital subtraction angiography (DSA) were performed in four and two patients respectively.

Imaging parameters used for various sequences were as follows: (1) repetition time (TR) ms/echo time (TE) msec, 375/11; flip angle, 90°; and matrix, 296 × 205 for spin-echo T1-W; (w) 3000/90; flip angle, 90°; and matrix, 492 × 479 for fast spin echo T2-W; and (3) 10000/125; 90°; and matrix, 300 × 205 for fluid-attenuated inversion recovery imaging. The other parameters were as follows: 5-mm section thickness with a 1.5-2.2 mm intersection gap and 230 mm × 250 mm field of view. Echo-planar DW MR imaging [2921/82.4 (b = 0 and 1000 s/mm^2)]; 24 sections; bandwidth, 2501 Hz per voxel; section thickness, 4 mm; intersection gap, 1.5-2.5 mm; field of view, 230 mm × 230 mm; matrix, 120 × 90; three signals acquired; voxel resolution, 2.05 mm × 2.53 mm × 4 mm) was performed in the axial plane before contrast material injection.

Diffusion weighted imaging was performed in 10 patients [apparent diffusion coefficient (ADC) values of 5 cases were listed in Table 1]. DW images were acquired at b value = 1000 mm^2/s in three orthogonal directions and combined into a trace image. DW images were visually inspected and classified as hyperintense, isointense and hypointense as compared with normal white matter. The mean ADC values (10^{-3} cm^2/s) were calculated on a voxel-by-voxel basis with the software incorporated into the MR imaging unit. Manual ROIs were placed using T2 weighted and contrast enhanced images as the guide.

A fat-suppression pulse was added to the axial T1-weighted sequences following contrast enhancement. The intravenous manual bolus dose of gadolinium based contrast medium given at 0.2 mL/kg (0.1 mmol/kg) body weight. T1-weighted 3D spin-echo sequences without fat suppression were performed with identical imaging parameters after contrast agent administration. Post contrast Spoiled Gradient Echo (SPGR) sequences were obtained using repetition time /echo time 5/10 ms; flip angle, 80; matrix, 492 × 479; slice thickness, 1 mm; slice interval, 0 and FOV, 240 × 240.

MRI images were reviewed by three neuroradiologists (R.K., R.M., AM.) by consensus agreements. Signal intensities in T1-W, T2-FSE and FLAIR were tabulated as hyper, hypo, isointensities. GRE and DWI sequences were assessed for blooming and restriction of dif-

Table 2 Mean apparent diffusion coefficient values in 5 patients

Case number	mean ADC (10^{-3} cm^2/s)
Case 1	1.98 ± 0.227
Case 2	1.67 ± 0.19
Case 3	1.184 ± 0.127
Case 7	2.774 ± 0.299
Case 9	1.54 ± 0.287
Mean	1.8296 ± 0.2038

ADC: Apparent diffusion coefficient.

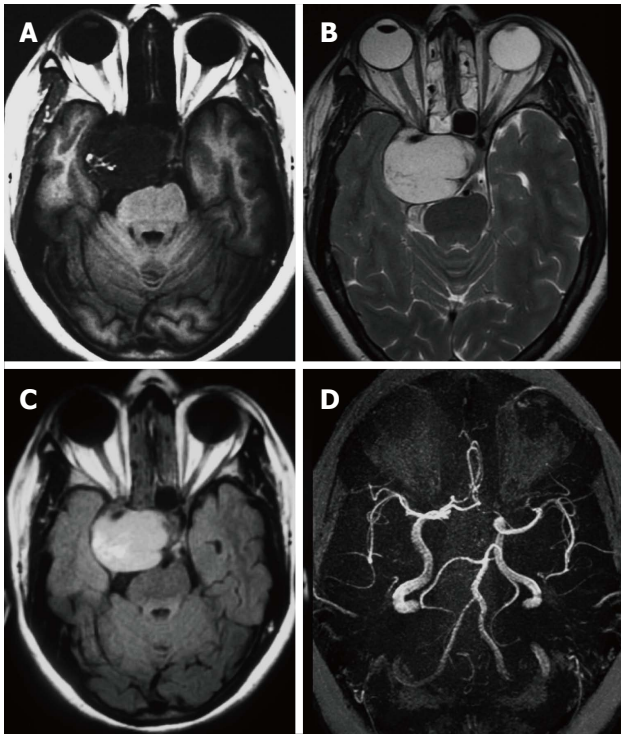

Figure 1 T1 weighted image, T2 weighted image and fluid-attenuated inversion recovery imaging images. A: Axial MRI image shows well defined lobulated hypointense mass on T1-W sequence image in the right cavernous sinus; B: Homogeneous hyperintensity of the mass is noted in the T2-W axial image; C: T2-W FLAIR axial image demonstrates marked hyperintense signal of the lesion; D: MRA reveals laterally stretched and displaced cavernous carotid segment. T1-W: T1 weighted image; T2-W: T2 weighted image; FLAIR: Fluid attenuated inversion recovery; MRI: Magnetic resonance imaging; MRA: Magnetic resonance angiography.

fusion. Degree of enhancement was noted from the contrast enhanced T1-Fat Suppressed sequences. The medical case files were reviewed retrospectively. The demography is detailed in Table 2. The age at presentation ranged from 13 to 63 years with a mean of 40.93 ± 13.82 years. There were 11 female and 4 male patients with a female preponderance. The mean age of female cohort was 42.27 ± 11.064 years. Diagnosis of cavernous hemangioma in the cavernous sinus was verified from the surgical and pathology notes. Eleven patients underwent surgical removal of the lesion and 2 patients had biopsy only. Diagnosis of CSH was confirmed histologically in 13 patients.

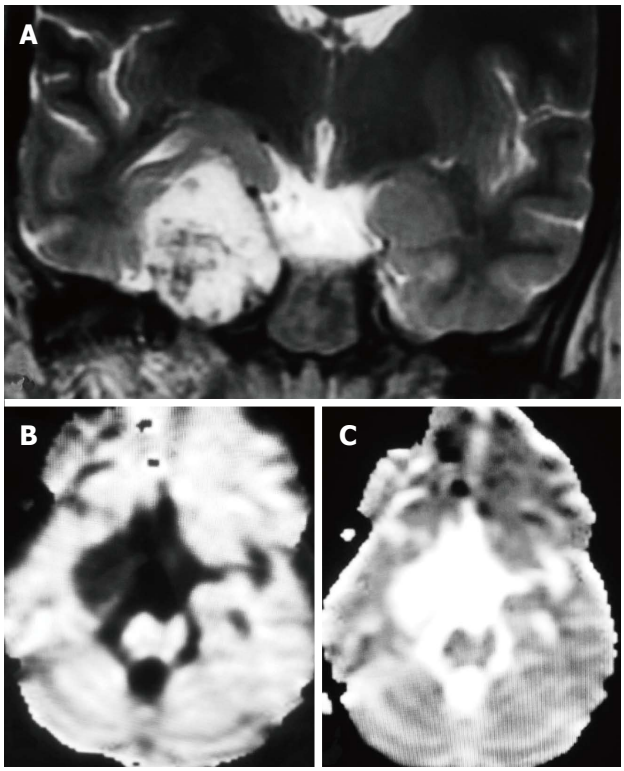

Figure 2 T2 weighted image coronal, diffusion-weighted imaging and apparent diffusion coefficient map images. A: T2-W coronal image demonstrates multiple flow voids within the CSH in the right cavernous sinus; B: DWI image shows hypointense signal on diffusion-weighted map (B) and corresponding hyperintensity on ADC maps (C) suggestive of facilitated diffusion. T2-W: T2 weighted image; CSH: Cavernous sinus hemangioma; DWI: Diffusion-weighted imaging; ADC: Apparent diffusion coefficient.

RESULTS

Headache was the constant feature and 7 patients had no visual symptoms despite large size of the lesion (Table 2). Papilledema was observed in one patient only. One patient had painful ophthalmoplegia in spite of a small sub-centimeter lesion occupying the small posterior segment of the cavernous sinus. Pre-operative MR imaging features are summarised in Table 3. Fourteen of the 15 patients showed well defined hypointense lesions occupying the cavernous sinus on T1-W imaging and all of these lesions showed homogeneous hyperintensity in T2-W and FLAIR imaging sequences (Figure 1). Significant extension beyond cavernous sinus into the Meckel's cave, prepontine cistern and impression onto the peduncle was seen in 14 of 15 patients and correlated with the presenting complaints.

In the ten patients who had DW imaging, hypointense signal on DWI images was a consistent finding suggestive of facilitated diffusion (Table 3, Figure 2). The ADC maps in these lesions were hyperintense in comparison with contralateral brain parenchyma and the mean ADC value (5 patients) was $1.82 \times 10^{-3} \pm 0.2186$ cm^2/s. GRE images in seven patients did not show any blooming (Figure 3). Intense enhancement of the lesion was noted in all patients (14 of 14). Centripetal

Table 3 Demography, clinical features, treatment and follow up

Case number	1[a]	2[a]	3[a]	4[a]	5	6	7	8	9	10	11	12	13	14	15
Age	51	26	38	47	52	63	26	33	59	51	50	34	38	33	13
Sex	F	M	F	F	F	F	F	F	M	M	F	F	F	F	M
Location	Right	Right	Left	Right	Left	Left	Right	Left	Right	Left	Right	Left	Left	Left	Left
Headache	1 yr	2 yr	Yes	4 yr	Yes	No	Yes	3 mo	Yes	Yes	Not available	No	No	6 mo	4 mo
Visual symptoms	Yes	12 mo	Blurring	6 mo	Nil	Nil	Blurring	Nil	6 mo	Nil	Not available	Nil	2 mo	6 mo	Nil
Cranial nerve involvement[b]	3rd, 4th, 6th	6th	No	3rd	No	3rd, 4th, 6th	No	No	No	6th	Not available	Numbness face	No	No	3rd, 6th
Operative details	Sub total	Sub total	Biopsy	Sub total	No surgery	Sub total	Biopsy	Sub total	No surgery	Complete excision	Sub total	Sub total	Sub total	Sub total	Complete excision
Follow up	No symptoms	No symptoms	No symptoms	No symptoms	No symptoms	Not available	No symptoms	No symptoms	Not available	No symptoms	Not available	No symptoms	No symptoms	No symptoms	No symptoms

[a]Received radiotherapy: Case no 1: 45 Gy in 25 fractions; case no 2: 25 Gy in 5 fractions; case 3: Stereotactic radiosurgery - 13 Gy in single fraction; case 4: Received adjuvant radiotherapy; [b]Cranial nerves 3 (oculomotor), 4 (trochlear), and 6 (abducens). F: Female; M: Male.

enhancement was observed progressively increasing in intensity in a young female patient. DSA examination demonstrated stretching and irregular narrowing of the internal carotid artery. Multiple venous channels were seen persisting in the venous phase (Figure 4). Contrast enhanced MRI performed after two years demonstrated significant shrinkage with thrombosis of the center of the lesion in one patient and total regression in another (Figure 5). Complete resection of CSH was possible in two patients (Figure 6). One patient had a sub-centimeter lesion in the left cavernous sinus presenting with painful ophthalmoplegia (Figure 7).

Three conspicuous imaging features were considered highly suggestive of the diagnosis: Homogeneous hyperintensity on T2-W sequences (14/15, 93.3%) facilitated diffusion (10/10, 100%) and intense contrast enhancement (14/14, 100%). Of the 13 patients who received surgery, subtotal excision or biopsy in 11 and complete excision in 2 patients were performed. Four patients received radiation therapy (Table 2). Eleven patients had serial follow-up ranging from 10 mo to 90 mo (mean 2.5 years) and all were asymptomatic on the serial follow-up.

DISCUSSION

Extracerebral CSH are rare in occurrence with a definite female preponderance. They are usually attached to the outer wall of cavernous sinus or located in the Meckel's cave or cerebellopontine angle[1,2]. Eleven of fifteen patients in our study were females and their preponderance is considered to be due to influence of estrogen. Symptoms are slow and insidious presenting with headaches, ophthalmoplegia, proptosis, cranial nerve palsy and endocrine disturbances[7,8]. In our series headache was the most common presenting complaint followed by vision abnormality and cranial nerve palsy. Imaging findings of meningiomas and schwannomas in this location overlap significantly. Typically, the lesion is not demonstrable on angiography in spite of the adjacent tortuous and serpentine arterial feeders and venous drainage. Degeneration into thrombosis, calcification, hyaline changes and hemorrhage are revealed by MR imaging[7-9].

Extension beyond cavernous sinus is noted in large lesions which may be seen also in meningioma, epidermoid, neurogenic tumors and granulomatous masses[3,7]. Extension beyond cavernous sinus was seen in all sizable lesions in our series and five lesions showed extensive para-cavernous extension. It was interesting to note, one of our CSH extended into the superior orbital fissure anteriorly, superiorly into the suprasellar region, greater wing of sphenoid bone and pterygoid fossa inferolaterally

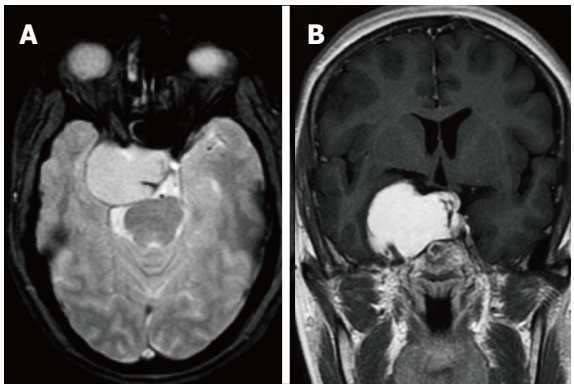

Figure 3 Axial gradient recalled echo and contrast enhanced T1 weighted image axial magnetic resonance images. A: Axial gradient recalled echo sequence does not show any blooming; B: Contrast enhanced coronal T1 weighted image shows intensely enhancing lesion encasing the internal carotid artery.

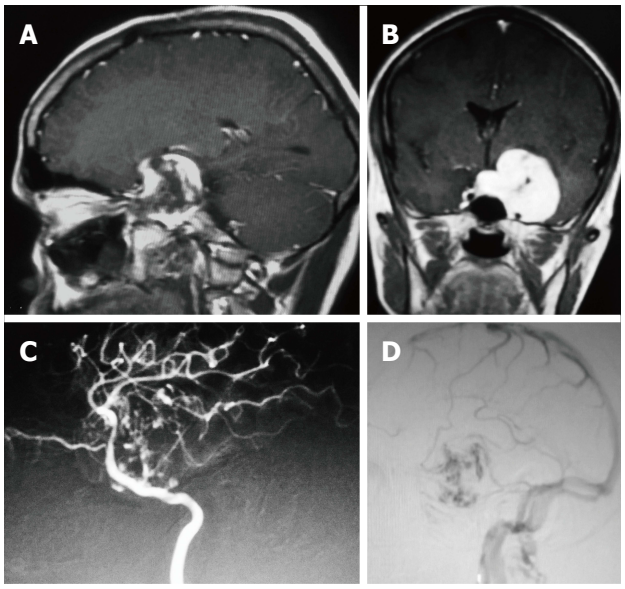

Figure 4 Contrast enhanced sagittal and coronal T1 weighted images and lateral views of digital subtraction angiography arterial and venous phases of left internal carotid angiogram. A, B: Centripetal filling of the CSH in the left cavernous sinus is demonstrated; C: Arterial phase of DSA shows diffuse irregularity and stretching of C3 to C5 segments; D: Venous phase shows stasis in the venous channels within the CSH. CSH: Cavernous sinus hemangioma; DSA: Digital subtraction angiography.

and into retroclival region posteriorly indistinguishable from a granulomatous or a neurogenic lesion[3,8]. Multiple cranial nerves and both internal carotid arteries traversing the cavernous sinus preclude complete surgical resection in addition to the risk of profuse bleeding. Tiny branches from the cavernous segment of the internal carotid artery may be revealed on digital subtraction angiography which are otherwise not appreciable on routine anatomical imaging[7,8]. Hypertrophied pial arteries, tumor stain and large draining veins were described in the intra-axial cavernous hemangioma closely resembling a highly vascular neoplasm[10,11].

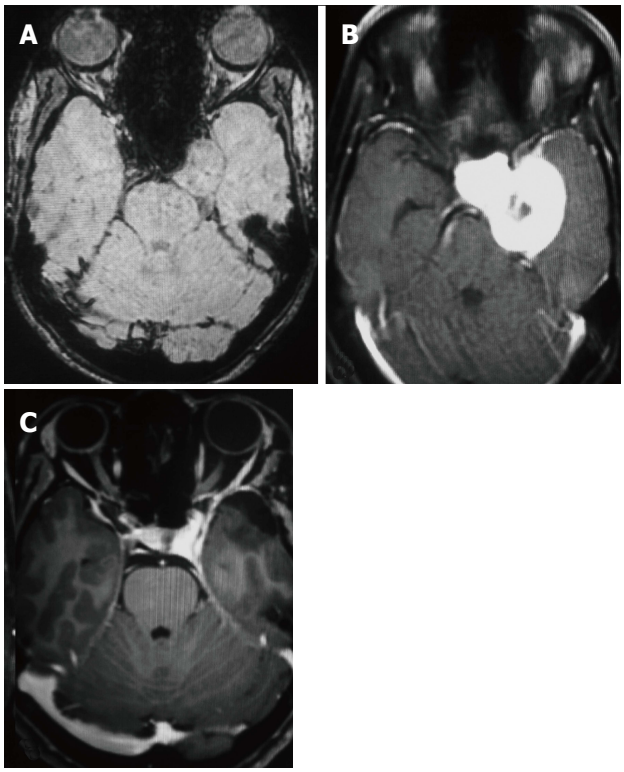

Figure 5 Contrast enhanced axial, susceptibility weighted imaging and 2 years follow up axial CE images. A: SWI axial image shows isointense signal of the CSH; B: Contrast enhanced axial T1-W image demonstrates the postero-inferior extension of the CSH; C: Two years post-operative surveillance axial contrast enhanced T1-W image shows complete resolution of the lesion. T1-W: T1 weighted image; SWI: Susceptibility weighted image; CSH: Cavernous sinus hemangioma.

On MR imaging, the lesions are seen as well-defined hypointense mass on T1-W and markedly hyperintense mass on T2-W sequence. In our series 14 of 15 patients (93%) showed these findings[3,4]. Schwannomas exhibit high signal intensity on T2-W and display heterogeneous enhancement following the expected course of the nerves from which they arise. Meningiomas show similar signal intensity to gray matter on T2-W unlike the CSH[3,12]. Delayed T1-W Gd-DTPA imaging confirms the temporal course of enhancement of the lesion. Uniformly intense and homogeneous contrast enhancement of all our CSH distinctly differ from the intra axial cavernous hemangiomas which mostly do not show enhancement[9,12,13]. Hypointense hemosiderin rim is not a common feature which is otherwise seen in intra-axial cavernous hemangioma. Bowing and displacement of the lateral wall of the cavernous sinus is clearly depicted on MR imaging indicating the extradural extension[5,12] and extensive extradural extension was seen in 5 patients in our series.

Lack of restriction to diffusion may be explained due to slow flow within the lesion which allows free diffusion of water molecules. There are no intervening neural/cellular elements outside the vascular channels which can prevent free movement of the protons and cause restriction of diffusion in the extravascular spaces

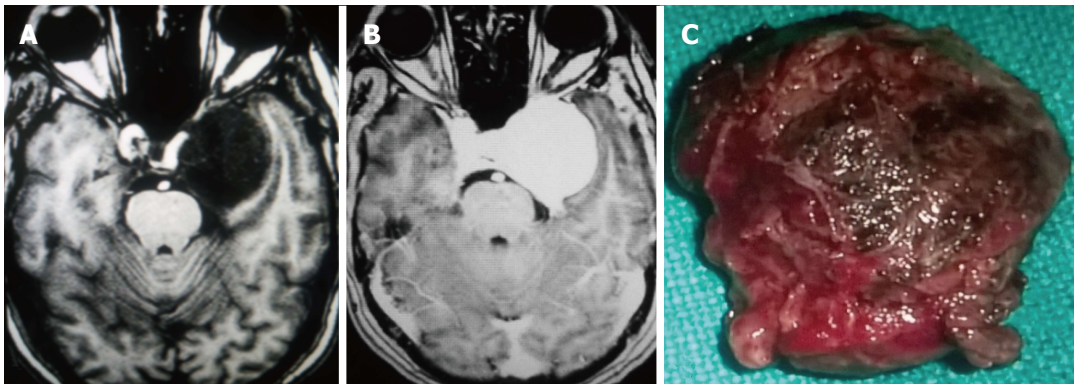

Figure 6 T1 weighted image plain, contrast enhanced axial magnetic resonance images and specimen photograph. A: Axial plain T1-W image shows large hypointense lesion in the left cavernous sinus; B: Contrast enhancement is intense in the axial T1-W image; C: The surgical specimen shows a well lobulated reddish mass resected entirely. T1-W: T1 weighted image.

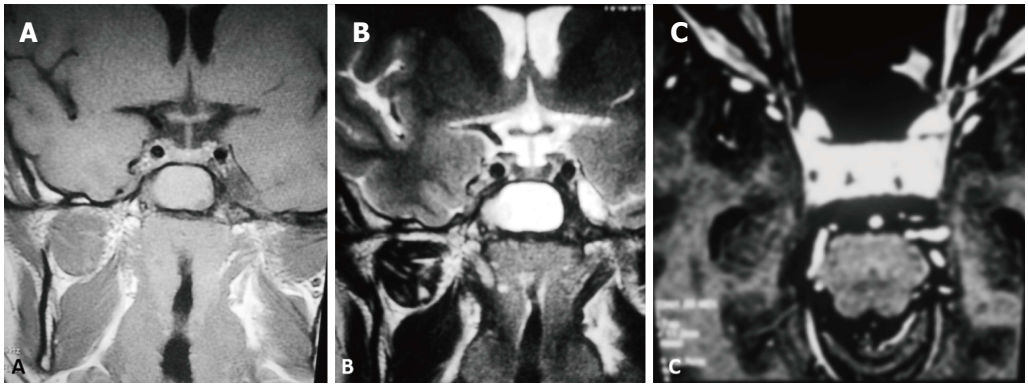

Figure 7 T2 weighted image coronal plain and contrast enhanced T1 weighted images. A: T1-W coronal unenhanced image shows an isointense to hypointense signal in the left cavernous sinus without affecting the internal carotid artery; B: Coronal T2-W shows small heterogeneous signal intensity in the left cavernous sinus; C: T1-W contrast enhancement shows homogeneous enhancement of the small lesion causing painful ophthalmoplegia. T1-W: T1 weighted image; T2-W: T2 weighted image.

as well. Hence these lesions are iso or hypointense to brain parenchyma on DWI images[4,14,15]. One hundred percent patients in our series showed hypointense signal on DW imaging suggesting facilitated diffusion (mean ADC = 1.8296 ± 0.2038 10^{-3} cm^2/s). Our series is the largest series which has looked into the incremental value of DW imaging in diagnosing CSH and results of our series suggest that facilitated diffusion is a consistent finding in CSH. However, at the *b* value = 1000 mm^2/s used in our series, effect of intravoxel incoherent motion is less though it cannot be eliminated completely which might have contributed to low signal on DWI and high ADC values[14,15]. False negative results may be seen in CSH with hemorrhage within and may cause a diagnostic dilemma, which was not seen in our series. CSH should be entertained in the differential diagnosis of a homogeneously enhancing cavernous sinus lesion that does not show evidence of hemorrhage and shows facilitated diffusion[15-17].

Blood flowing in the CSH is not exactly venous blood as it has not passed through a tissue and hence there is no oxygen extraction. Since the blood within the CSH behaves as oxygenated blood there is no susceptibility induced signal loss on SWI imaging, as noted in our series. Similar signal intensities are observed in the cavernous hemangioma elsewhere in the body, unless there are phleboliths or thrombosed areas[9,13,14]. Hemorrhage has been reported in CSH[18]. Concentric layers of hemosiderin are the hallmark of intra-axial lesions due to recurrent hemorrhages into the wall of the lesion causing slow growth. None of the cases in our series showed this finding. At least two thirds of cavernous hemangiomas exhibit some degree of vascular blush unlike the parenchymal cavernous angiomas which are occult to catheter angiography[8,10,12]. Microscopically CSH consists of multiple vascular channels lined by a single layer of endothelium without muscular layer. In our series, vascular blush was noted from distal branches of middle meningeal artery and meningeal branches of internal carotid artery in 3 patients while one lesion was avascular on DSA as reported by Krief *et al*[19]. Delayed SPECT imaging of the red blood pool scintigrams demonstrate increased activity persistently in contrast to the photopenic areas in meningioma, chordoma and chondrosarcoma[18,19].

Sclerosing CSH is a less aggressive solid/semisolid entity in the spectrum of lesions of the cavernous sinus.

Aversa do Souto *et al*[20] and Shi *et al*[21] successfully operated a less aggressive CSH in the cavernous sinus by internal decompression without any life-threatening intraoperative bleeding similar to the case 10 in this series. Connective tissue proliferation between the vascular spaces evolves into a more densely packed solid or semisolid sclerosing Type-B CSH over a period of time. On imaging the subtype B of CSH is hyperintense on T2W and shows heterogeneous contrast enhancement while subtype-A is soft and pulsatile having thin walled blood spaces with a propensity to bleed profusely during surgery. Due to the abundant vascularization of these lesions, surgery is extremely complex and is associated with high morbidity such as cranial neuropathies[20,22]. CSH respond to radiation unlike the extraaxial cavernous angiomas. Gamma Knife surgery is a safe and effective primary as well as adjuvant treatment modality for CSH[23,24]. In one series the reported post-therapy shrinkage of CSH using gamaknife surgery was reported to be 84.6% at 12 mo follow-up[25]. Two-year follow-up of four patients in this series after stereotactic radiotherapy were asymptomatic. The mean follow-up in our series was 2.5 years and all patients had no symptoms over the serial follow-up. However, there are limitations of this study, as this was a retrospective study of a relatively small sample size we could not estimate the inter observer variability.

MR imaging findings reported in this study are characteristic and diagnostic of CSH. T1-W hypointensity, homogeneous hyperintensity on T2-W sequences, intense enhancement following gadolinium injection and facilitated diffusion on DW imaging establish the diagnosis prior to surgery. Absence of hemosiderin within the lesion on GRE with facilitated diffusion significantly increases the diagnostic accuracy. With the characteristic and favourable MR imaging evidence followed by an open biopsy, attempt for radical excision is unwarranted since CSH responds well to stereotactic radiation.

COMMENTS

Background

Even though magnetic resonance imaging (MRI) is the modality of choice for characterising lesions at the cavernous sinus, the diagnosis of a cavernous hemangioma can still be in doubt, with the main differential diagnosis being a schwannoma of the V nerve or meningioma.

Research frontiers

The study aimed to elucidate the clinical, MRI, pathological features of these lesions and asses the incremental value of diffusion-weighted imaging (DWI) in diagnosing them.

Innovations and breakthroughs

This is one of the largest series of cavernous sinus hemangiomas that have clinical-radiological and pathological correlation as well as follow-up details. The study also highlights the incremental value of DWI imaging and the apparent diffusion coefficient value in these lesions which has not elucidated in the existing literature.

Applications

T1-weighted hypointensity with homogeneous hyperintensity on T2-weighted sequence, absence of hemosiderin within the lesion on GRE sequence and intense post contrast enhancement favour the diagnosis of cavernous sinus hemangioma (CSH). On DW imaging CSH shows facilitated diffusion and is nearly 100% specific for CSH. Markedly hypointense hemangioma on T1W images suggests schirrous nature of the lesion and are amenable to complete surgical excision.

Terminology

Cavernous hemangioma in the cavernous sinus has an estimated prevalence of 1% incidence. The lesion is rare in occurrence closely mimicking commonly encountered cavernous sinus lesions such as schwannoma, meningioma, chordoma, granuloma, carotid aneurysm and lympho-proliferative conditions. Microscopically cavernous sinus hemangioma (CSH) consist of multiple vascular channels lined by a single layer of endothelium without muscular layer without any intervening neural tissue. Diffusion weighted MR imaging measures the diffusivity of the water molecules in the tissue. Hindrance of water molecule movement is gives a hyperintense signal on diffusion imaging interpreted as restricted diffusion and indicates high cellularity of the tissue. CSH shows facilitated diffusion on DWI.

Peer-review

Cavernous sinus hemangiomas (CSHs) is a benign vascular malformation which belong to Intracranial-extraaxial cavernous hemangiomas. Radiosurgery can effectively control the growth of smaller CSHs. Diagnosing CSH preoperatively is very important, but its radiological differential diagnosis is difficult. In this paper, the MRI sequence is abundant. Especially the number of DWI cases has a large proportion, which can provide valuable information for the diagnosis of CSH.

REFERENCES

1 **Simard JM**, Garcia-Bengochea F, Ballinger WE, Mickle JP, Quisling RG. Cavernous angioma: a review of 126 collected and 12 new clinical cases. *Neurosurgery* 1986; **18**: 162-172 [PMID: 3960293 DOI: 10.1227/00006123-198602000-00008]

2 **Del Curling O**, Kelly DL, Elster AD, Craven TE. An analysis of the natural history of cavernous angiomas. *J Neurosurg* 1991; **75**: 702-708 [PMID: 1919691 DOI: 10.3171/jns.1991.75.5.0702]

3 **Razek AA**, Castillo M. Imaging lesions of the cavernous sinus. *AJNR Am J Neuroradiol* 2009; **30**: 444-452 [PMID: 19095789 DOI: 10.3174/ajnr.A1398]

4 **Yadav RR**, Boruah DK, Yadav G, Pandey R, Phadke RV. Imaging characteristics of cavernous sinus cavernous hemangiomas. *Neuroradiol J* 2012; **25**: 515-524 [PMID: 24029085 DOI: 10.1177/197140091202500503]

5 **Sohn CH**, Kim SP, Kim IM, Lee JH, Lee HK. Characteristic MR imaging findings of cavernous hemangiomas in the cavernous sinus. *AJNR Am J Neuroradiol* 2003; **24**: 1148-1151 [PMID: 12812943]

6 **Yao Z**, Feng X, Chen X, Zee C. Magnetic resonance imaging characteristics with pathological correlation of cavernous malformation in cavernous sinus. *J Comput Assist Tomogr* 2006; **30**: 975-979 [PMID: 17082705 DOI: 10.1097/01.rct.0000221953.06135.3e]

7 **Zhou LF**, Mao Y, Chen L. Diagnosis and surgical treatment of cavernous sinus hemangiomas: an experience of 20 cases. *Surg Neurol* 2003; **60**: 31-36; discussion 36-37 [PMID: 12865008 DOI: 10.1016/S0090-3019(03)00190-3]

8 **Linskey ME**, Sekhar LN. Cavernous sinus hemangiomas: a series, a review, and an hypothesis. *Neurosurgery* 1992; **30**: 101-108 [PMID: 1738435 DOI: 10.1227/00006123-199201000-00018]

9 **Gonzalez LF**, Lekovic GP, Eschbacher J, Coons S, Porter RW, Spetzler RF. Are cavernous sinus hemangiomas and cavernous malformations different entities? *Neurosurg Focus* 2006; **21**: e6 [PMID: 16859259 DOI: 10.3171/foc.2006.21.1.7]

10 **Rao VR**, Pillai SM, Shenoy KT, Radhakrishnan VV, Mathews G. Hypervascular cavernous angioma at angiography. *Neuroradiology* 1979; **18**: 211-214 [PMID: 530433 DOI: 10.1007/BF00345728]

11 **Numaguchi Y**, Kishikawa T, Fukui M, Sawada K, Kitamura K,

Matsuura K, Russell WJ. Prolonged injection angiography for diagnosing intracranial cavernous hemangiomas. *Radiology* 1979; **131**: 137-138 [PMID: 424574 DOI: 10.1148/131.1.137]
12 **McEvoy SH**, Farrell M, Brett F, Looby S. Haemangioma, an uncommon cause of an extradural or intradural extramedullary mass: case series with radiological pathological correlation. *Insights Imaging* 2016; **7**: 87-98 [PMID: 26385689 DOI: 10.1007/s13244-015-0432-y]
13 **Jinhu Y**, Jianping D, Xin L, Yuanli Z. Dynamic enhancement features of cavernous sinus cavernous hemangiomas on conventional contrast-enhanced MR imaging. *AJNR Am J Neuroradiol* 2008; **29**: 577-581 [PMID: 18065511 DOI: 10.3174/ajnr.A0845]
14 **Korchi AM**, Cuvinciuc V, Caetano J, Becker M, Lovblad KO, Vargas MI. Imaging of the cavernous sinus lesions. *Diagn Interv Imaging* 2014; **95**: 849-859 [PMID: 23763988 DOI: 10.1016/j.diii.2013.04.013]
15 **Ginat DT**, Mangla R, Yeaney G, Ekholm S. Diffusion-weighted imaging of skull lesions. *J Neurol Surg B Skull Base* 2014; **75**: 204-213 [PMID: 25072014 DOI: 10.1055/s-0034-1371362]
16 **Bansal S**, Suri A, Singh M, Kale SS, Agarwal D, Sharma MS, Mahapatra AK, Sharma BS. Cavernous sinus hemangioma: a fourteen year single institution experience. *J Clin Neurosci* 2014; **21**: 968-974 [PMID: 24524951 DOI: 10.1016/j.jocn.2013.09.008]
17 **Mathur A**, Jain N, Kesavadas C, Thomas B, Kapilamoorthy TR. Imaging of skull base pathologies: Role of advanced magnetic resonance imaging techniques. *Neuroradiol J* 2015; **28**: 426-437 [PMID: 26427895 DOI: 10.1177/1971400915609341]
18 **Salanitri GC**, Stuckey SL, Murphy M. Extracerebral cavernous hemangioma of the cavernous sinus: diagnosis with MR imaging and labeled red cell blood pool scintigraphy. *AJNR Am J Neuroradiol* 2004; **25**: 280-284 [PMID: 14970031]
19 **Krief O**, Sichez JP, Chedid G, Bencherif B, Zouaoui A, Le Bras F, Marsault C. Extraaxial cavernous hemangioma with hemorrhage. *AJNR Am J Neuroradiol* 1991; **12**: 988-990 [PMID: 1950936]
20 **Aversa do Souto A**, Marcondes J, Reis da Silva M, Chimelli L. Sclerosing Cavernous Hemangioma in the Cavernous Sinus: Case Report. *Skull Base* 2003; **13**: 93-99 [PMID: 15912165 DOI: 10.1055/s-2003-820564]
21 **Shi J**, Hang C, Pan Y, Liu C, Zhang Z. Cavernous hemangiomas in the cavernous sinus. *Neurosurgery* 1999; **45**: 1308-1313; discussion 1308-1313 [PMID: 10598697 DOI: 10.1097/00006123-199912000-00006]
22 **Anqi X**, Zhang S, Jiahe X, Chao Y. Cavernous sinus cavernous hemangioma: imaging features and therapeutic effect of Gamma Knife radiosurgery. *Clin Neurol Neurosurg* 2014; **127**: 59-64 [PMID: 25459244 DOI: 10.1016/j.clineuro.2014.09.025]
23 **Tang X**, Wu H, Wang B, Zhang N, Dong Y, Ding J, Dai J, Yu T, Pan L. A new classification and clinical results of Gamma Knife radiosurgery for cavernous sinus hemangiomas: a report of 53 cases. *Acta Neurochir* (Wien) 2015; **157**: 961-969; discussion 969 [PMID: 25862173 DOI: 10.1007/s00701-015-2417-5]
24 **Wang Y**, Li P, Zhang XJ, Xu YY, Wang W. Gamma Knife Surgery for Cavernous Sinus Hemanginoma: A Report of 32 Cases. *World Neurosurg* 2016; **94**: 18-25 [PMID: 27373416 DOI: 10.1016/j.wneu.2016.06.094]
25 **Park CK**, Choi SK, Kang IH, Choi MK, Park BJ, Lim YJ. Radiosurgical considerations for cavernous sinus hemangioma: long-term clinical outcomes. *Acta Neurochir* (Wien) 2016; **158**: 313-318 [PMID: 26658989 DOI: 10.1007/s00701-015-2657-4]

P- Reviewer: Chowdhury FH, Xie Q **S- Editor**: Song XX
L- Editor: A **E- Editor**: Lu YJ

Published by **Baishideng Publishing Group Inc**
7901 Stoneridge Drive, Suite 501, Pleasanton, CA 94588, USA
Telephone: +1-925-223-8242
Fax: +1-925-223-8243
E-mail: bpgoffice@wjgnet.com
Help Desk: http://www.f6publishing.com/helpdesk
http://www.wjgnet.com